

Redshift Evolution of the Underlying Type Ia Supernova Stretch Distribution

N. Nicolas ^{★1}, M. Rigault ^{★★2},

Y. Copin¹, R. Graziani², G. Aldering³, M. Briday¹, J. Nordin, Y.-L. Kim¹, Saul Perlmutter³, and G. Smadja¹

¹ Université de Lyon, F-69622, Lyon, France; Université de Lyon 1, Villeurbanne; CNRS/IN2P3, Institut de Physique des Deux Infinis, Lyon

² Université Clermont Auvergne, CNRS/IN2P3, Laboratoire de Physique de Clermont, F-63000 Clermont-Ferrand, France.

³ Physics Division, Lawrence Berkeley National Laboratory, 1 Cyclotron Road, Berkeley, CA, 94720

Received 2 November 1992 / Accepted 7 January 1993

ABSTRACT

The true nature of type Ia supernovae (SNe Ia) remains largely unknown, and as ~~measure of~~ survey statistics increase, the question of astrophysical systematic uncertainties rises, ~~and~~ notably that of the SN Ia population redshift drift. In this paper, we study the redshift evolution of SN Ia SALT2.4 lightcurve stretch, a purely intrinsic SN property, to probe this drift. The SN stretch has been shown to strongly correlate with the SN's environment, ~~and~~ notably with stellar age tracers. Following the evolution of fraction of young and old SNe Ia as predicted by Rigault et al. (2018), and assuming non-drifting ~~→constant/stationary?~~ underlying stretch distribution for each population, model the expected SN Ia stretch distribution as a function of redshift. We test our prediction against data from the literature chosen to have negligible selection effects to ensure that any observed drift is indeed astrophysical and not observational. We clearly demonstrate that the underlying SNe Ia stretch distribution is evolving as a function of redshift, and that the young/old drifting model is a much better description of the data than any non-drifting model, including the sample-based asymmetric distributions used by the Beams with Bias Correction algorithm to correct Malmquist bias. Our favored underlying stretch model is bimodal: a high-stretch mode shared by both young and old environments, and a low-stretch mode exclusive to old environments. ~~The underlying SNe Ia population is evolving as a function of redshift. This is purely a repetition of a previous sentence – see new sentence – and the exact impact on cosmology remains to be studied. The precise impact of the redshift evolution of the underlying SNe Ia population on cosmology remains to be studied.~~ Yet, the astrophysical drift of the SN stretch distribution does affect current Malmquist bias corrections and thereby distances derived from SN affected by selection effects. We highlight that such a bias will increase with surveys covering larger redshift ranges, which is particularly important for LSST.

Key words. Cosmology – Type Ia Supernova – Systematic uncertainties

1. Introduction

*YC: you should run a grammar corrector, e.g. **grammaly**. e.g. "SNe dichotomy" vs. "SN dichotomy", "analysis" vs. "analyses", etc. By the way, as we capitalize "Fig." before a reference, shouldn't we capitalize "Section" before reference?*

Type Ia supernovae (SNe Ia) are powerful cosmological distance indicators that have enabled the discovery of the acceleration of the Universe's expansion (Riess et al. 1998; Perlmutter et al. 1999). They remain today a key cosmological probe to understand the properties of dark energy (DE) as it is the only tool able to precisely map the recent expansion rate ($z < 0.5$), when DE is driving it (e.g. Scolnic et al. 2019). They also are key to directly measure the Hubble Constant (H_0), provided one can calibrate their absolute magnitude (Riess et al. 2016; Freedman et al. 2019). Interestingly, the value of H_0 derived when the SNe Ia are anchored on Cepheids (the SH0ES project, Riess et al. 2009, 2016) is $\sim 5\sigma$ higher than what is predicted from cosmic microwave background (CMB) data measured by Planck assuming the standard Λ CDM ~~ref? isn't it at the end of the sentence? Do you think it should be before the "or"?~~, or when the SN luminosity is anchored at intermediate redshift by the baryon acous-

tic oscillation (BAO) scale (Riess et al. 2019; Reid et al. 2019; Planck Collaboration et al. 2018; Feeney et al. 2019). While using the tip of the red giant branch technique in place of the Cepheids seem to favor an intermediate value of H_0 (Freedman et al. 2019, 2020), time delay measurements from strong lensing seem to also favor high H_0 values (Wong et al. 2019).

The H_0 tension has received a lot of attention, as it could be a sign of new fundamental physics. Yet, no simple solution is able to accommodate this H_0 tension when accounting for all other probes (Knox & Millea 2019) and ~~the current most promising one currently possible~~ scenario appears to be a burst of expansion at the matter-radiation decoupling moment caused by a (fine tuned) early dark energy (Poulin et al. 2019). *I don't see the point of going into this debate...*

Alternatively, systematic effects affecting one or several of the aforementioned analyses could also explain the tension. Rigault et al. (2015) suggested that SNe Ia from the Cepheid calibrator sample differ by construction from the Hubble flow sample ones as ~~it they? the former~~ strongly favors young stellar populations ~~environments where one could find Cepheids~~. This selection effect would impact the derivation of H_0 if SNe Ia from young and older environments differ in average standardized magnitudes.

[★] n.nicolas@ipnl.in2p3.fr, equal contribution

^{★★} m.rigault@ipnl.in2p3.fr, equal contribution

For the last decades, numerous analyses have studied the relation between SNe Ia and host properties, finding first that the standardized SNe Ia magnitude significantly depends on the host stellar mass, SNe Ia from high-mass host being brighter on average (e.g. Kelly et al. 2010; Sullivan et al. 2010; Childress et al. 2013; Betoule et al. 2014; Rigault et al. 2018; Kim et al. 2019). This mass-step correction is currently used in cosmological analyses (e.g. Betoule et al. 2014; Scolnic et al. 2018), including for deriving H_0 (Riess et al. 2016, 2019). Yet, the underlying connection between the SNe and their host remains unclear when using global properties such as the host stellar mass, which raises the question of the accuracy of the correction. More recently, studies have used the local SN environment to probe more direct connections between the SN and its environments (Rigault et al. 2013), showing that local age tracers such as the Local specific Star Formation Rate (LsSFR) or the local color are more strongly correlated with the standardized SN magnitude (Rigault et al. 2018; Roman et al. 2018; Kim et al. 2018), suggesting age as the driving parameter underlying the mass-step. If true, this would have a significant impact for cosmology, *not only because there would be a redshift drift magnitude correction to apply, but also because it might strongly vary just the existence of a redshift-drift mag. correction is of importance here, even if it does not vary now taken into account* (Rigault et al. 2013; Childress et al. 2014; Scolnic et al. 2018). Yet, the importance of local SN environmental studies remains highly debated (e.g. Jones et al. 2015, 2019) and especially the impact it *what does ‘it’ refer to, the ‘importance’? no, to the SN environment. Do you think it needs rephrasing?* has on the derivation of H_0 (Jones et al. 2015; Riess et al. 2016, 2018; Rose et al. 2019).

Shouldn’t this paragraph, introducing the concept of old and young populations and LsSFR, be moved here? I agree. Now done.

The concept of the SNe Ia age dichotomy arose with the study of the SN Ia rate. Mannucci et al. (2005); Scannapieco & Bildsten (2005); Sullivan et al. (2006); Aubourg et al. (2008) have shown that the relative SNe Ia rate in galaxies could be explained if two populations existed, one young, following the host star formation activity, and one old following the host stellar mass (the so called “prompt and delayed” or “A+B” model). In Rigault et al. (2018) we used the LsSFR (specific Star Formation Rate at the SN location) to classify which are the younger (those with a high LsSFR) and which are the older (those with low LsSFR). Furthermore, since the first SNe Ia host analyses, the SN stretch has been known to be strongly correlated with the SN host properties (Hamuy et al. 1996, 2000), *correlation that which what does this “which” refer to? is that better?* has been extensively confirmed since (e.g. Neill et al. 2009; Sullivan et al. 2010; Lampeitl et al. 2010; Kelly et al. 2010; Gupta et al. 2011; D’Andrea et al. 2011; Childress et al. 2013; Rigault et al. 2013; Pan et al. 2014; Kim et al. 2019). Following the “A+B” model and the connection between SN stretch and host properties, Howell et al. (2007) first discussed the potential redshift drift of the SN stretch distribution. In this paper we revisit this analysis with the most recent SNe Ia dataset.

In this paper, we take a step aside to probe the validity of our modeling of the SN population, which we claim to be constituted of two age-populations (Rigault et al. 2013; Rigault et al. 2015, 2018): one old and one younger, the former having on average lower lightcurve stretches and being brighter after standardization. We use the correlation between the SN age, as probed by local specific star formation rate (Rigault et al. 2018), and the SN stretch to model the expected evolution of the underlying SN stretch distribution as a function of redshift. This modeling re-

lies on three assumptions: (1) there are two distinct populations of SNe Ia; (2) the relative fraction of each of these populations as a function of redshift follows the model presented in Rigault et al. (2018) and (3) the underlying distribution of stretch for each age sample *is constant is a fixed model* and does not significantly evolve with time. This paper aims at testing this specific model with datasets from the literature.

We present in section 2 the sample we are using for this analysis, derived from the Pantheon catalog (Scolnic et al. 2018). We discuss the importance of obtaining a “complete” sample, i.e. representative of the true underlying SNe Ia distribution, and how we build one from the Pantheon sample. We then present in section 3 our modeling of the distribution of stretch, *using as a function of redshift-based models for the stretch distribution of young and old SNe Ia what??? rephrase Is that better?*. Our results are presented in section 4, where we test whether the SN stretch distribution evolves as a function of redshift and if the aforementioned age model is in good agreement with this evolution. Consequences for cosmology of our results are briefly discussed in section 5.1 and we conclude in section 6.

2. Complete Sample Construction

We base our analysis on the most recent *comprehensive* *What does it mean? Are there SNe Ia compilation that are not comprehensive?* SNe Ia compilation, the Pantheon catalog from Scolnic et al. (2018). A naive approach to test the SN stretch redshift drift would be to simply compare the observed SN stretch distributions in a few bins of redshift. In practice, however, *differential* *Do you mean “different”, or that it is based on differences (the definition of “differential” as given by my search engine)?* selection effects are affecting the observed SN stretch distributions. Indeed, because the observed SN Ia magnitude correlates with the lightcurve stretch (and color), the first SNe Ia that a magnitude-limited survey will miss are the lowest-stretch (and reddest) ones. Consequently, if magnitude-related selection effects are not accounted for, one might confuse true population drift with survey properties, and conversely.

Assuming sufficient (and unbiased) spectroscopic follow-up for acquiring typing and host redshift, the selection effects of magnitude-limited surveys should be negligible below a given redshift at which even the faintest SNe Ia can be observed. In contrast, targeted surveys have highly complex selection functions and will be discarded from our analysis. Fortunately, modern SN cosmology samples such as the Pantheon one are now dominated by magnitude-limited surveys.

We present in Fig. 1 the lightcurve stretch and color of SNe Ia from the following surveys: PanStarrs (PS1 Rest et al. 2014), the Sloan Digital Sky Survey (SDSS Frieman et al. 2008) and the SuperNovae Legacy Survey (SNLS Astier et al. 2006). An ellipse in the SALT2.4 (x_1, c) plane with $x_1 = \pm 3$ and $c = \pm 0.3$ encapsulates the full distribution (Guy et al. 2007; Betoule et al. 2014); see also Bazin et al. (2011) and Campbell et al. (2013) for similar contours, the second using a more conservative $|c| \leq 0.2$ cut. Assuming the SN absolute magnitude with $x_1 = 0$ and $c = 0$ is $M_0 = -19.36$ (Kessler et al. 2009; Scolnic et al. 2014), we can derive the absolute standardized magnitude at maximum of light $M = M_0 - \alpha x_1 + \beta c$ along the aforementioned ellipse given the standardization coefficient $\alpha = 0.156$ and $\beta = 3.14$ from Scolnic et al. (2018): the faintest SN Ia is that with ($x_1 = -1.65, c = 0.25$) and an absolute standardized magnitude at peak in Bessel B band of $M_{min}^{l_0} = -18.31$ mag. Since one ought to detect this object typically *a week 5 days before and 40 days a week* after peak to build a suitable lightcurve, the effec-

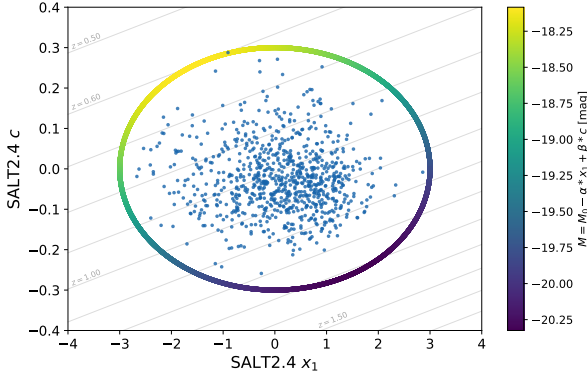


Fig. 1. SALT2.4 stretch (x_1) and color (c) lightcurve parameters of SNe Ia from the SDSS, PS1 and SNLS samples of the Pantheon catalog. The individual SNe are shown as blue dots and a 2D histogram is shown in gray to highlight point density. *I don't think it's really needed Ok, changed. Better?*. The ellipse ($x_1 = \pm 3, c = \pm 0.3$) is displayed, colored by the corresponding standardized absolute magnitude using the α and β coefficients from Scolnic et al. (2018). The grey diagonal lines represent the (x_1, c) evolution for $m = m_{lim}$, for z between 0.50 and $z = 1.70$ using SNLS's m_{lim} of 24.8 mag.

tive limiting standardized absolute magnitude is approximately $M_{lim} = -18.00$ mag. Hence, given the magnitude limit m_{lim} of a magnitude limited survey, one can derive the maximum redshift z_{lim} above which the faintest SNe Ia will be missed using the relation between apparent magnitude, redshift and absolute magnitude $\mu(z_{lim}) = m_{lim} - M_{lim}$.

SNLS typically acquires SNe Ia in the redshift range $0.4 < z < 0.8$; at these redshifts, the rest-frame Bessel B band roughly corresponds to the SNLS i filter, that has a 5σ depth of 24.8 mag¹. This converts to a $z_{lim} = 0.60$, in agreement with Neill et al. (2006), Perrett et al. (2010) and Bazin et al. (2011). Fig. 14 of Perrett et al. (2010) suggests a lower limit of $z_{lim} = 0.55$; both limits will be considered, as discussed below.

Similarly, PS1 observes SNe Ia in the range $0.2 < z < 0.4$, their g -band 5σ depth is 23.1 mag (Rest et al. 2014), which yields to $z_{lim} = 0.30$ in agreement with, e.g., Fig. 6 of Scolnic et al. (2018). This figure is also suggestive of a more conservative $z_{lim} = 0.27$.

In a similar redshift range, SDSS has a limiting magnitude of 22.5 (Dilday et al. 2008; Sako et al. 2008), which would lead to a $z_{lim} = 0.24$. However, the SDSS surveys were more sensitive to limited spectroscopic resources; Kessler et al. (2009) pointed out that during the first year of SDSS, SNe Ia with $r - mag < 20.5$ were favored for spectroscopic follow-up, corresponding to a redshift cut at 0.15. For the rest of the SDSS survey, additional spectroscopic resources were available, and Kessler et al. (2009) and Dilday et al. (2008) show a relative completeness *what is a relative completeness???* In Dilday 2008, they give a median redshift of $\langle z \rangle = .22$ for spectroscopically confirmed SNe Ia up to $z_{lim} = 0.2$. Following these analyses, we will use $z_{lim} = 0.2$ as the baseline SDSS redshift limit.

~~For the rest of the analysis, we will consider the aforementioned redshift limits, as well as more conservative values for each of these surveys, namely $z_{lim} = 0.15$ for SDSS, $z_{lim} = 0.27$ for PS1 and $z_{lim} = 0.55$ for SNLS. why do you remind the conservative values, and not the fiducial ones? Just refer to Table 1.~~

Table 1. Composition of the SNe Ia dataset used in this analysis. Conservative cuts are indicated in brackets.

Survey	z_{lim}	N_{SN}
SNf	–	114
SDSS	0.20 (0.15)	167 (82)
PS1	0.30 (0.27)	160 (122)
SNLS	0.60 (0.55)	102 (78)
HST	–	26
Total	–	569 (422)

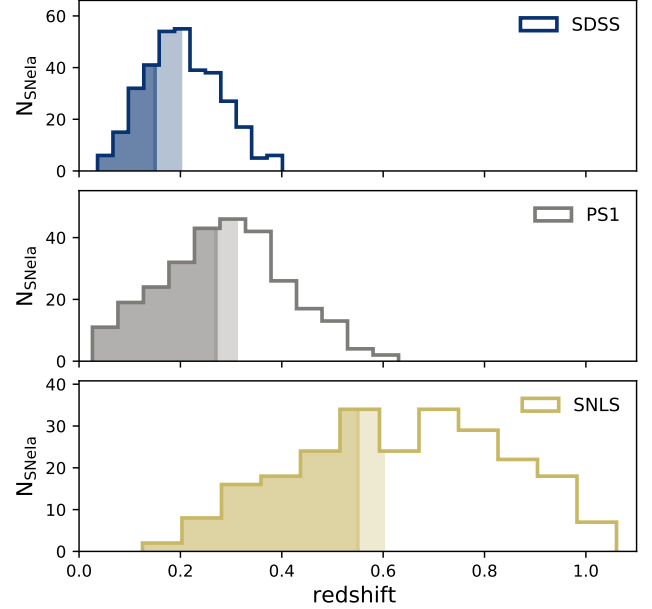


Fig. 2. From top to bottom: Redshift histograms of SNe Ia from the SDSS, PS1 and SNLS dataset respectively (data from Pantheon, Scolnic et al. 2018). The colored parts represent the distribution of SNe Ia kept in our analysis for they are supposedly free from selection bias (see section 2). The darker (resp. lighter) color responds to the conservative (resp. fiducial) selection cut.

The complete sample selection is summarized in Table 1, and the redshift distribution of these three surveys is shown in Fig. 2. As expected, the selected redshift limits roughly correspond to the peak of these histograms.

In addition, we use the SNe Ia from the Nearby Supernova Factory (SNfactory, Aldering et al. 2002) published in Rigault et al. (2018) and that have been discovered from non-targeted searches (114 SNe Ia, see their sections 3 and 4.2.2; *SNe Ia time series are published in ? should add Aldering in prep. and Pander in prep. as suggested by Greg*). The spectroscopic follow-up was done over a redshift range of $0.02 < z < 0.09$ (as in Rigault et al. 2018), while the search was much deeper. As such, these SNe Ia are assumed to be a random sampling of the underlying SN population. The SNfactory sample is particularly useful for studying SN property drift, as it enables us to have a large SN Ia sample at $z < 0.1$.

Finally, we include the HST sample from Pantheon, that similarly have a search deeper than the follow-up and that we therefore kept entirely (Strolger et al. 2004).

We present the stretch distribution and redshift histogram of these five surveys up to their respective z_{lim} in Fig. 3. *The combined samples' mean stretches in bins of redshift is also presented in Fig. 5, where we see that when considering selection-*

¹ CFHT final release website.

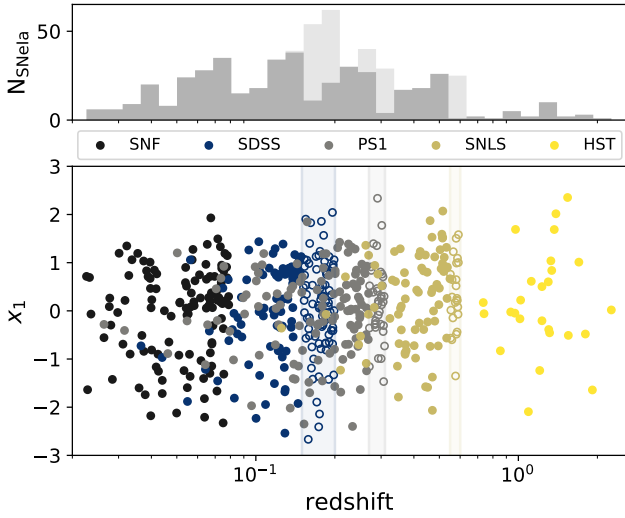


Fig. 3. Bottom: SALT2.4 lightcurve stretch as a function of redshift for each survey considered in this analysis (see legend). Solid (resp. open) markers correspond to the conservative (resp. fiducial) redshift cuts. Top: combined redshift histogram in dark (resp. light) gray for the conservative (resp. fiducial) redshift cuts.

bias-free SN Ia samples, SNe Ia at higher redshift have on average larger stretch (0.34 ± 0.10 at $z \sim 0.65$) than those at lower redshift (-0.17 ± 0.10 at $z \sim 0.05$). That is the evolution that we attempt to model in the next section. *Last part added following Yannick's comment about the fact that this result is model-independent; see last paragraph before section 3.2*

You should also present/refer to Fig.5, showing the significant evolution of mean stretch as function of z in complete samples. Next Sec. aims at modeling this evolution. Done.

3. Modeling the redshift drift

Rigault et al. (2018) presented a model for the evolution of the fraction of younger and older SNe Ia as a function of redshift following former work on rates and delay time distributions (e.g., Mannucci et al. 2005; Scannapieco & Bildsten 2005; Sullivan et al. 2006; Aubourg et al. 2008; Childress et al. 2014; Maoz et al. 2014). In short, it was assumed that the number of “young” SNe Ia follows the star formation rate (SFR) in the Universe, while the number of “old” SNe Ia follows the number of Gyr-old stars in the Universe, i.e. the stellar mass (M^*). Hence, if we denote $\delta(z)$ (resp. $\psi(z) = 1 - \delta(z)$) the fraction of young (resp. old) SNe Ia in the Universe as a function of redshift, then the ratio δ/ψ is expected to follow the evolution of the specific star formation rate (SFR/M^*), which goes as $(1+z)^{-2.8}$ until $z \sim 2$ (e.g., Tasca et al. 2015). Since $\delta(0.05) \sim \psi(0.05)$ (Rigault et al. 2013; Rigault et al. 2018; Wiseman et al. 2020), in agreement with rate expectations (Mannucci et al. 2006; Rodney et al. 2014), Rigault et al. (2018) concluded that

$$\delta(z) = \left(K^{-1} \times (1+z)^{-2.8} + 1 \right)^{-1} \quad (1)$$

with $K = 0.87$. This model is comparable to the evolution predicted by Childress et al. (2014) based on SN rates in galaxies depending on their quenching time as a function of their stellar mass.

3.1. “Base” underlying stretch distribution

There is a generic confusion between “SN stretch” (individual SN, as in Eq.3/4) and something like “SN stretch distribution” (population, as in Eq.2). This is confusing...

To model the evolution of the global SN stretch distribution as a function of redshift, given our aforementioned model of the evolution of the fraction of younger and older SNe Ia with redshift cosmic time *Is it really common to call z the “cosmic time”? What does this modification bring to the understanding of this evolution? We might make the confusion between the “age” of a SNe, and the “time” of its explosion given by the redshift..., we need to model the SN stretch distribution for each age subsample. That paragraph sounds like a tautology... Added “global” so that we see its meaning*

I suggest we remove the use of “we” when referring to previous papers, like “In R+18, we did...” to be replaced by “R+18 did...” That has been a recurring question. This paper is part of a series of paper, so it seemed ok, but for that I’ll trust the common way, though I feel like lying by making it sound impartial when we actually use “our” results. People should know that we take our previous work as a baseline.

Rigault et al. (2018) presented the relation between SN stretch and LsSFR measurement, a progenitor age tracer, using the SNfactory sample. This relation is shown in Fig. 4 for the SNfactory SNe used in the current analysis. Given the structure of the stretch-LsSFR scatter plot, our model of the underlying SN Ia stretch distribution is defined as follows:

- for the younger population (i.e., $\log(\text{LsSFR}) \geq -10.82$), the stretch distribution is modeled as a single normal distribution $\mathcal{N}(\mu_1, \sigma_1^2)$;
- the older population (i.e., $\log(\text{LsSFR}) < -10.82$) stretch distribution is modeled as a bimodal Gaussian mixture $a \times \mathcal{N}(\mu_1, \sigma_1^2) + (1 - a) \times \mathcal{N}(\mu_2, \sigma_2^2)$, where one mode is the same as for the young population, a representing the relative influence of the two modes.

When combined to the previously described prediction of the evolution of younger SNe Ia as a function of redshift (Eq. 1), our model $X_1(z)$ for the underlying stretch distribution as a function of redshift is written

$$X_1(z) = \delta(z) \times \mathcal{N}(\mu_1, \sigma_1^2) + (1 - \delta(z)) \times \left[a \times \mathcal{N}(\mu_1, \sigma_1^2) + (1 - a) \times \mathcal{N}(\mu_2, \sigma_2^2) \right]. \quad (2)$$

In fact, not clear what this eq. does here: it is supposed to be superseded by Eq.3/4. Maybe it should be moved to Sec.3.1.2 when we use $\delta(z)$ as a proxy to y^i . It should not! The evolution as a function of z doesn’t depend on how we determine the parameters. This is what people should use for the “Base” model, and then there are two ways to get the parameters. If you think there is a clearer way for people to understand this, please tell us. All 3 eq. (2), (3) and (4) are of the same importance and are used in the .py we wrote.

The maximum-likelihood estimate of the 5 free parameters $\theta \equiv (\mu_1, \mu_2, \sigma_1, \sigma_2, a)$ of the model is obtained by minimizing the following pseudo- χ^2 :

$$-2 \ln(L) = -2 \sum_i \ln \mathcal{P}(x_1^i | \theta; dx_1^i, y^i), \quad (3)$$

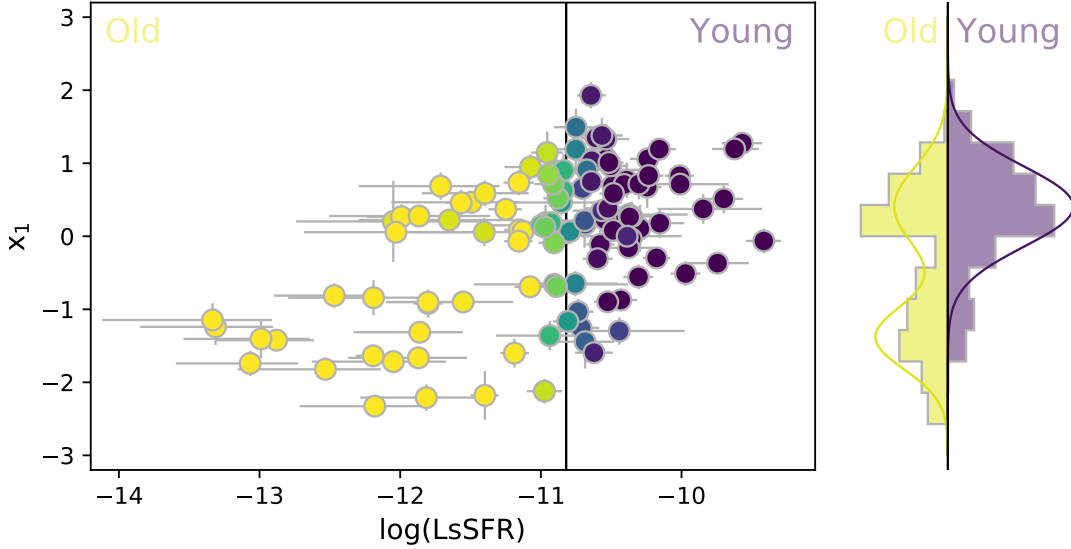


Fig. 4. *Main:* SALT2.4 lightcurve stretch (x_1) as a function of the local specific star formation rate (LsSFR) for SNfactory SNe used in this analysis. The color corresponds to the probability, p_y , for the SNe Ia to be young, i.e. to have $\log \text{LsSFR} \geq -10.82$ (see Rigault et al. 2018). *Right:* p_y -weighted histogram of the SN stretches, as well as the adjusted Base model; the younger and older population contributions are shown in purple and yellow, respectively.

with

$$\mathcal{P}(x_1^i | \theta; dx_1^i, y^i) = y^i \times \mathcal{N}(x_1^i | \mu_1, \sigma_1^2 + dx_1^{i2}) + (1 - y^i) \times \left[a \times \mathcal{N}(x_1^i | \mu_1, \sigma_1^2 + dx_1^{i2}) + (1 - a) \times \mathcal{N}(x_1^i | \mu_2, \sigma_2^2 + dx_1^{i2}) \right], \quad (4)$$

where i is the index of the SN Ia, x_1^i , dx_1^i and y^i are the SALT2.4 stretch, its associated error and the probability that the SN is young, respectively. In practice, to ensure fraction a is constrained between 0 and 1, we fit for α such that $a = \arctan(\alpha)/\pi + 0.5$, ~~which results in an asymmetric error on a . Given the fact that 1. it's barely asymmetric ($a \sim 0.5$), 2. no one cares, it should be symmetrized (quadratically). Probably σ errors are not symmetric either! Mickaël, do you have arguments to maintain an asymmetric definition of a ?~~

Depending on whether y^i can be estimated directly from LsSFR measurements or not, there are two ways to proceed, which we now discuss.

3.1.1. With LsSFR measurements

For the SNfactory sample, we can readily set $y^i = p_y^i$, the probability to have $\log \text{LsSFR} \geq -10.82$ (see Fig. 4), to minimize Eq. 3 with respect to θ . Results on fitting the SNf SNe with this model are shown Table 2 and illustrated in Fig. 4.

3.1.2. Without LsSFR measurements

When lacking direct LsSFR measurements (i.e. p_y^i), we can extend the analysis to non-SNfactory samples by using the redshift-evolution of the fraction $\delta(z)$ of young SNe Ia (Eq. 1) as a proxy for the probability of a SN to be young. This still corresponds to minimizing Eq. 3 with respect to the parameters $\theta \equiv (\mu_1, \mu_2, \sigma_1, \sigma_2, a)$ of the stretch distribution X_1 (Eq. 2), but this time assuming $y^i = \delta(z^i)$ for any given SN i .

For the rest of the analysis, we will therefore minimize Eq. 3 using p_y^i – the probability for the SN i to be young – when available (i.e. for SNfactory dataset), and $\delta(z^i)$ – the expected fraction of young SNe Ia at the SN redshift z^i – otherwise.

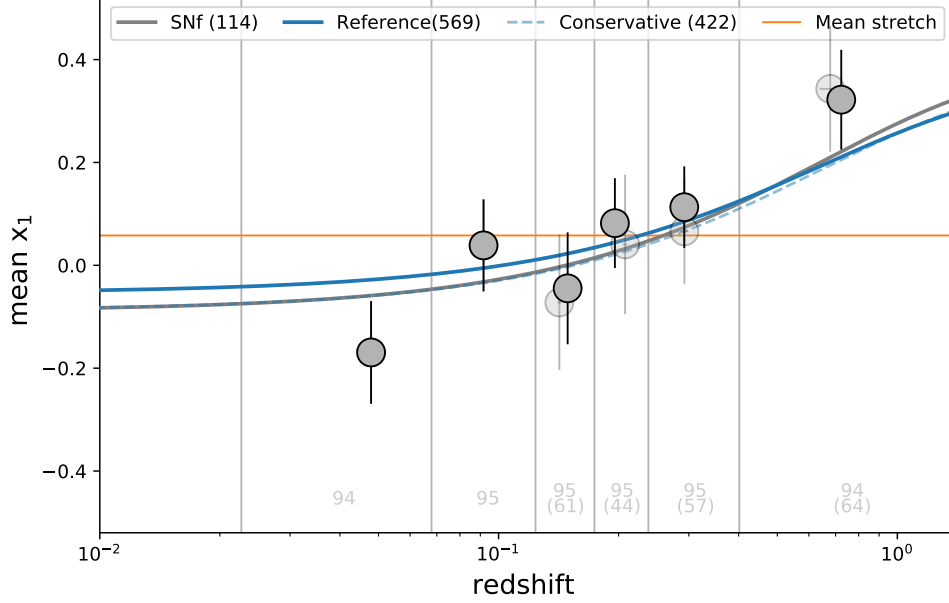
Results of fitting this model to all the 569 (resp. 422) SNe from the fiducial (resp. conservative) sample are given Table 2, and the predicted redshift evolution of mean stretch (mean of Eq. 2) illustrated in Fig. 5. *I'm confused: grey points in Fig.5 are model independent, aren't they? Only the curve is related to the model. Yes. What is confusing?* We see in this figure that the measured mean SN Ia stretch per bin of redshift, defined so that each contain an equal number of SNe of the fiducial sample, closely follows our redshift drift modeling; that is, ~~when considering selection-bias-free SN Ia samples, SNe Ia at higher redshift have on average larger stretch (0.34 ± 0.10 at $z \sim 0.65$) than those at lower redshift (-0.17 ± 0.10 at $z \sim 0.05$), and namely that SNe Ia at higher redshift have a larger average stretch (0.34 ± 0.10 at $z \sim 0.65$) than those at lower redshift (-0.17 ± 0.10 at $z \sim 0.05$). This is model-independent, and a nice result by itself, and should be already mentioned right at the end of Sec.2. I agree. I dumbly copied that right before Sec.3, and reworded that part for a reminder.~~ This is indeed what is expected if old environments favor low SN stretches (e.g. Howell et al. 2007) and if the fraction of old SNe Ia declines as a function of redshift. See section 4 for a more quantitative discussion.

3.2. Alternative models

In section 3.1, we have modeled the underlying stretch distribution following Rigault et al. (2018), i.e. as a single Gaussian for the “young” SNe Ia and a mixture of two Gaussians for the “old” SNe Ia population, one being the same as for the young population, plus another one for the fast-declining SNe Ia that seem to only exist in old local environments. This is our so-called “Base” model. However, to test different modeling choices, we have implemented a suite of alternative parametrizations that we also adjust to the data following the procedure described in section 3.1.2.

Table 2. Best fit values of the parameters for the Base stretch distribution model when applied to the SNfactory dataset only (114 SNe Ia), the fiducial 569 SN Ia sample or the conservative one (422).

Sample	μ_1	σ_1	μ_2	σ_2	a
SNfactory	0.41 ± 0.08	0.55 ± 0.06	-1.38 ± 0.10	0.44 ± 0.08	$0.48^{+0.08}_{-0.08}$
Fiducial	0.37 ± 0.05	0.61 ± 0.04	-1.22 ± 0.16	0.56 ± 0.10	$0.51^{+0.09}_{-0.10}$
Conservative	0.38 ± 0.05	0.60 ± 0.04	-1.26 ± 0.13	0.53 ± 0.08	$0.47^{+0.09}_{-0.08}$

**Fig. 5.** Evolution of the mean SN SALT2.4 stretch (x_1) as a function of redshift. Markers show the mean stretch measured in redshift bins of equal sample size, indicated in light gray at the bottom of each redshift bins. Full and light markers are used when considering the fiducial or the conservative samples, respectively. The orange horizontal line represents the mean stretch of the fiducial sample, illustrating the expectation if the SN stretch distribution is not evolving with redshift. Best fits of our Base drifting model are shown as blue, dashed-blue and gray, when fitted on the fiducial sample, the conservative one or the SNfactory dataset only, respectively; all are compatible. The light-blue band illustrates the amplitude of the error of the best fit model when considering the fiducial dataset.

Howell et al. (2007) used a simpler unimodal model per age category, assuming a single normal distribution for each of the young and old populations. We thus consider a “Howell+drift” model, with one single Gaussian per age group and the $\delta(z)$ drift from Eq. 1.

Alternatively, since we aim at probing the existence of an evolution with redshift, we also test constant models by restricting the “Base” and “Howell” models to use a supposedly redshift-independent fraction $\delta(z) \equiv f$ of young SNe; these models are hereafter labeled “Base+constant” and “Howell+constant”.

We also consider another intrinsically non-drifting model, the one developed for Beams with Bias Correction (BBC, Scolnic & Kessler 2016; Kessler & Scolnic 2017), used in recent SN cosmological analyses (e.g. Scolnic et al. 2018; Abbott et al. 2019; Riess et al. 2016, 2019) to account for Malmquist biases. The BBC formalism assumes sample-based (hence intrinsically non-drifting) asymmetric Gaussian stretch distributions: $\mathcal{N}(\mu, \sigma_-^2 \text{ if } x_1 < \mu, \text{ else } \sigma_+^2)$. The idea behind this sample-based approach is twofold: (1) Malmquist biases are driven by survey properties and (2) since current surveys cover limited redshift ranges, doing so *what? having a sample-based approach* covers some potential redshift evolution information (Scolnic & Kessler 2016; Scolnic et al. 2018). See further discussion concerning BBC in section 5.1.

Finally, for the sake of completeness, we also consider simple the “Gaussian” and “Asymmetric” Gaussian non-drifting models.

4. Results

We adjusted each of the models described above on both the fiducial and conservative samples (cf. section 2); results are gathered in Table 3, and illustrated in Fig. 6.

Since the various models have different degrees of freedom, we use the Akaike Information Criterion (AIC, e.g. Burnham & Anderson 2004) to compare their ability to properly describe the observations. This estimator penalizes extra degrees of freedom to avoid over-fitting the data, and is defined as follow:

$$\text{AIC} = -2 \ln(L)_{\min} + 2k \quad (5)$$

where $-2 \ln(L)_{\min}$ is the minimum value of the pseudo- χ^2 as defined Eq. (3), and k is the number of free parameters to be adjusted. The reference model is the one with the smallest AIC; in comparison to this model, the models with $\Delta\text{AIC} < 5$ are coined acceptable, the ones with $5 < \Delta\text{AIC} < 20$ are unfavored, and those with $\Delta\text{AIC} > 20$ are deemed excluded. This roughly corresponds to 2, 3 and 5 σ limits for a Gaussian probability distribution.

We first note that the best model (with smallest AIC) is the so-called Base model, implementing the Rigault et al. (2018)

Table 3. Comparison of the relative ability of each model to describe the data. For each considered model, we report if the model is drifting or not, its number of free parameters and, for both the fiducial and the conservative cuts, the pseudo- χ^2 , $-2 \ln(L)$ (see Eq. 3), the AIC and the AIC difference (ΔAIC) between this model and the Base model used as reference for it has the lowest AIC.

Name	drift	k	Fiducial sample (569 SNe)			Conservative sample (422 SNe)		
			$-2 \ln(L)$	AIC	ΔAIC	$-2 \ln(L)$	AIC	ΔAIC
Base	$\delta(z)$	5	1456.7	1466.7	–	1079.5	1089.5	–
Howell+drift	$\delta(z)$	4	1463.3	1471.3	–4.6	1088.2	1096.2	–6.7
Asymmetric	–	3	1485.2	1491.2	–24.5	1101.3	1107.3	–17.8
Howell+const	f	5	1484.2	1494.2	–27.5	1101.2	1111.2	–21.7
Base+const	f	6	1484.2	1496.2	–29.5	1101.2	1113.2	–23.7
BBC-like	per sample	3×5	1468.2	1498.2	–31.5	1083.6	1113.6	–24.1
Gaussian	–	2	1521.8	1525.8	–59.1	1142.6	1146.6	–57.1

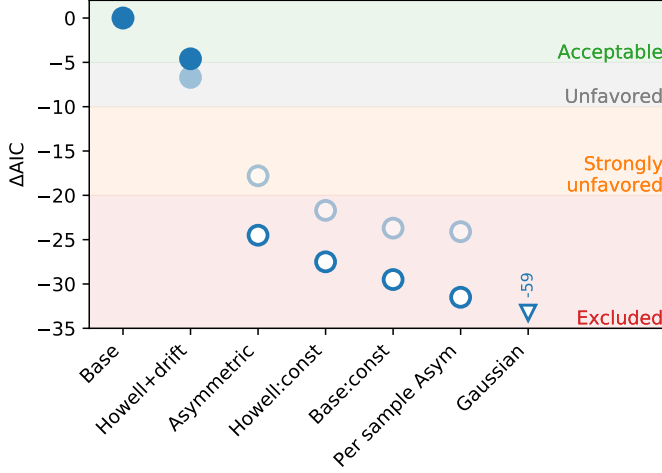


Fig. 6. ΔAIC between “Base” model (reference) and other models (see Table 3). Full and open blue markers correspond to models with and without redshift drift, respectively. Light markers show the results when the analysis is performed on the conservative sample rather than the fiducial one. Color-bands illustrate the validity of the models, from Acceptable ($\Delta AIC > -5$) to Excluded ($\Delta AIC < -20$), see text. According to the AIC, all non-drifting models (open symbols) are excluded to be as good a representation of the data as the Base (drifting) model.

description of the stretch distribution and its redshift evolution. This is therefore the reference model, both on the fiducial *some-where, you still use the “ref. sample” terminology! corrected, thanks.* and conservative samples.

Furthermore, we find that redshift-independent stretch distributions are all excluded as *uitable* descriptions of the data relative to the Base model. In fact, the best non-drifting model (the Asymmetric one) has a very marginal chance ($p \equiv \exp(\Delta AIC/2) = 5 \times 10^{-6}$) to describe the data as well as the Base model. This result is just a quantitative assessment of qualitative facts clearly visible in Fig. 5: the mean SN stretch per bin of redshift strongly suggests a significant redshift evolution rather than a constant value, and this evolution is well described by Eq. 1.

Surprisingly, the sample-based Gaussian asymmetric modeling used by current implementations of the BBC technique (Scolnic & Kessler 2016; Kessler & Scolnic 2017), is one of the worst modelisations of our analysis (see section 4). While its pseudo- χ^2 is the smallest of all redshift-independent models (but still $\Delta\chi^2 = -11.5$ worse than the reference Base model), it is strongly penalized for requiring 15 free parameters (μ_0, σ_{\pm} for each of the 5 samples of the analysis). We report in Table 4 the samples’ μ_0 and σ_{\pm} adjusted on the *nominally* selection-free

Table 4. Best-fit parameters for our sample-based asymmetric modeling of the underlying stretch distribution.

Asymmetric	σ_-	σ_+	μ_0
SNfactory	1.34 ± 0.13	0.41 ± 0.10	0.68 ± 0.15
SDSS	1.31 ± 0.11	0.42 ± 0.09	0.72 ± 0.13
PS1	1.01 ± 0.11	0.52 ± 0.12	0.38 ± 0.16
SNLS	1.41 ± 0.13	0.15 ± 0.13	1.22 ± 0.15
HST	0.76 ± 0.36	0.79 ± 0.35	0.11 ± 0.44

samples using our fiducial cuts (see section 2). We find our results in close agreement with Scolnic & Kessler (2016) for SNLS and SDSS and with Scolnic et al. (2018) for PS1, who derived these model parameters using the full BBC formalism, using numerous simulations to model the selection effects (see details e.g., section 3 of Kessler & Scolnic 2017). The agreement between our fit of the asymmetric Gaussians on the supposedly selection-free part of the samples and the results derived using the BBC formalism supports our approach to get a sample with negligible selection effects. *It’s not very clear what you mean to convey in this sentence. Basically, because we get the same results but with a different approach, theirs being complicated and supposedly good for selection effects, we think it can show that ours (using the limiting magnitude blablabla) is at least as good.*

We further discuss the consequence of this result for cosmology in section 5.

For the sake of robustness *?????*, we also performed tests allowing the high-stretch mode of the old population to differ from the young population mode, hence adding two degrees of freedom. The corresponding fit is not significantly better, with a ΔAIC of -0.4 ; this strengthens the fact that the young and old populations indeed appear to share the same underlying high-stretch mode. We also allowed the young population to have a low-stretch mode *Well I didn’t! But I strongly think we should, as well as Martin, Jakob and now Greg too. We’ve let the 3 Gaussians to have independant μ s and σ s, but never the young having the low-stretch, unless you did at some point. If so, it should be addressed earlier and compared, because Fig. 4 invites us to think it does.,* finding its amplitude to be compatible with 0 ($< 2\% \pm ???$).

5. Discussion

To the best of our knowledge, the SN Ia stretch redshift drift has never been explicitly accounted for in cosmological analyses, though bayesian hierarchy formalism such as UNITY (Rubin et al. 2015), BAHAMAS (Shariff et al. 2016) or Steve (Hinton et al. 2019) can easily allow it. Not doing so is a second order issue for SN cosmology, as it only affects the way one accounts

for Malmquist bias. *I don't understand why you say it's a 2nd order effect if all samples are significantly Malmquist biased!?. Yes, but is it taken into account?* Indeed, as long as Phillip Tripp right?'s relation *ref?* standardization parameter α is not intrinsically redshift dependent (a study behind the scope of this paper, but see e.g. Scolnic et al. 2018), the stretch-corrected SNe Ia magnitudes used for cosmology are blind to the underlying stretch distribution for complete samples *Why is that? Even for sample not "complete", if α doesn't depend on z , $\alpha * x_1$ won't see the underlying distribution, right?* However, all modern surveys do have significant Malmquist bias at least for the upper half of their SN redshift distribution. As a consequence, an ill-modeling of the underlying stretch distribution will bias the derived SN magnitude for these *these what? These surveys. Reword?* (see e.g., Rubin et al. 2015; Rubin & Hayden 2016). The fact that the currently-used sample-based asymmetric Gaussian distribution modeling is excluded as being as good as our drifting model is worrisome and is further discussed in the next sections. *I don't see the point of this kind of sentence... I guess that if the most common tool is biased, it has to be addressed, and this serves as a transition, but I think we could just go into the subsection directly.*

5.1. BBC formalism and underlying stretch distributions

IMHO, you should take care of not converting this paper into an anti-BBC paper: just show the results, and let people make their opinion. Furthermore, I find this paragraph mostly a repetition of previous statements and results... Probably.

The commonly used tool for doing Malmquist bias correction in SN cosmology is the BBC formalism described in Scolnic & Kessler (2016) and Kessler & Scolnic (2017), which is used in recent SN cosmological analyses (Jones et al. 2018; Scolnic et al. 2018; Brout et al. 2019; Abbott et al. 2019) including the direct measurement of H_0 (Riess et al. 2016, 2019). *This all have already been said before, there's no point at repeating it IMHO. Maybe just a simpler introductory sentence without all the references? The first part yes, but not the second. See proposed paragraph below.*

The BBC formalism previously mentioned is used in some recent SN cosmological analyses (Jones et al. 2018; Scolnic et al. 2018; Brout et al. 2019; Abbott et al. 2019) including the direct measurement of H_0 (Riess et al. 2016, 2019). Yet, as shown in Section 4, their sample-based asymmetric Gaussian distribution modeling is excluded as being as good as our drifting model.

Yet, the current underlying stretch modeling of the BBC formalism, a sample-based asymmetric Gaussian distribution, is excluded to be an as good representation of the data than our Base drifting modeling, see section 4. *Again, unnecessary repetition. Here, I agree. I moved this part in the previous paragraph.* Then, unlike what Scolnic & Kessler (2016, section 2) and Scolnic et al. (2018, section 5.4) suggested, *the fact that traditional surveys span limited redshift ranges, the per-sample approach cannot correctly account for implicit redshift drifts namely that a per-sample approach might be able to account for unmodeled redshift drift thanks to the limited redshift span of traditional surveys, the results indicate that it is far from being as useful as directly modeling the redshift drift. I don't understand what they suggested and what is wrong... Rephrase. Done.* We stress here that, as measurements of modern surveys try to cover increasingly larger redshift ranges in order to reduce calibration systematic uncertainties, this sample-based approach *which*

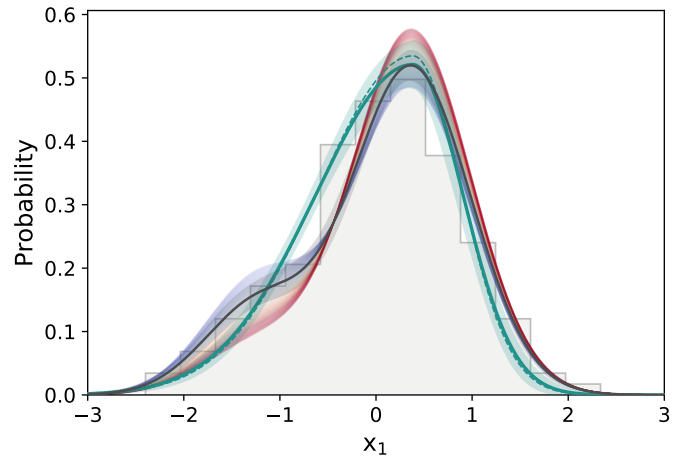


Fig. 7. Distribution of the PS1 SN Ia SALT2 .4 stretch (x_1) after the fiducial redshift limit cut (grey histogram). This distribution is supposed to be a random draw from the underlying stretch distribution. The green line shows the BBC model of this underlying distribution (asymmetric Gaussian). The full line (band) is our best fit (its error); the dashed line shows the Scolnic et al. (2018) result. The black line (band) show our best fitted Base-modeling (its error, see Table 2) that includes redshift drift. For illustration, we show as colored (from blue to red with increasing redshifts) the evolution of the underlying stretch distribution as a function of redshift for the redshift range covered by PS1 data.

one? Done. is becoming less valid, notably for PS1, DES and, soon, LSST. Already with current surveys, the BBC sample-based technique is ruled out at representing the data as well as our best model: $\Delta\text{AIC} < -20$, which could be interpreted as a probability $p = 2 \times 10^{-7}$ of being an as good representation of the data as the Base model. *Again, unnecessary repetition. I think that with the rewording I done, it's ok. I don't find anything else to put after "a probability of ...".* Note that even considering the SNfactory dataset like any other (i.e., ignoring the LsSFR measurements, see section 3), reduces this difference to $\Delta\text{AIC} < -10$, still strongly disfavoring the modeling currently used as part of the sample-based formalism this modeling. If we were to use Scolnic & Kessler (2016) and Scolnic et al. (2018) best fit values of the μ_0, σ_{\pm} asymmetric parameters for SNLS, SDSS and PS1, respectively *which parameters? Now precised.*, the ΔAIC between our Base drifting model and the BBC modeling would go even deeper from -32 to -47 . *But you would be using parameters derived specifically for incomplete samples on specially-constructed complete sample: what is the validity of the comparison??? Well their parameters are made for incomplete samples, but taking into account the selection effects; we got rid of them, so technically, the underlying parameters should both represent those of the underlying distribution.*

5.2. First step toward quantification of the cosmological impact of inaccurate stretch distribution modeling.

We illustrate in Fig. 7 the prediction difference in the underlying stretch distribution between the BBC modeling and our Base drifting model for the PS1 sample. Our model is bimodal and the relative amplitude of each mode depends on the redshift-dependent fraction of old and young SNe Ia in the sample: the higher the fraction of old SNe Ia (at lower redshift), the higher the amplitude of the old-specific low-stretch mode. This redshift dependency is shown as blue to red underlying distributions in Fig. 7 for redshift ranges covered by PS1. The observed x_1 his-

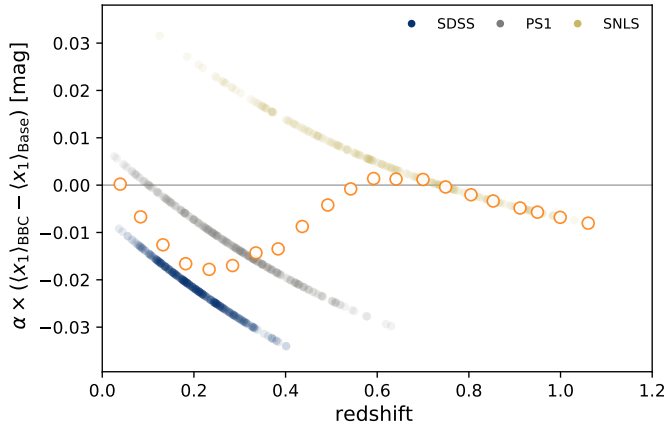


Fig. 8. Difference of mean stretch standardization (in mag, using $\alpha = 0.156$ from Scolnic et al. 2018) between the BBC algorithm and our Base drifting model, as a function of redshift, considering the SDSS, PS1 and SNLS datasets. The colored markers show the difference for SDSS, PS1 and SNLS samples (see legend) considering the individual SN redshifts (no redshift cut applied). The orange markers represent their mean evolution in 30 regularly-spaced redshift bins.

togram, in grey, corresponds to the sum of individual underlying SN-redshift distributions, represented by the black line. *Not clear: you mean the black curve – a model – or the histogram – an observation? Is it clearer?* As expected, the two approaches *which ones? the BBC modeling and our Base drifting model, as introduced in the paragraph. Do you think we should repeat it? I feel that we’ve been talking about BBC vs. Base for so long it would be too much:* strongly differ in modeling the negative part of the SN stretch distribution. The BBC asymmetric distribution goes through the middle of the bimodal distribution, over-estimating the number of SNe Ia at $x_1 \sim -0.7$ and under-estimating it at $x_1 \sim -1.7$ in comparison to our Base drifting model for typical PS1 SN redshifts. *This is definitely not obvious from the Fig. solely... I agree that both distributions are quite close to the histogram. Our black line may be closer to the bins at low redshift, that the green line is way too high at -0.9, but ours is way too low at 0.5 or so.* This means that the bias-correction of individual SN stretches, δ_{x_1} (Kessler & Scolnic 2017), and consequently the magnitude bias correction, μ_B , is most likely inaccurate and redshift dependent.

The amplitude of this magnitude bias for cosmology is beyond the scope of this paper given the complexity of the BBC analysis. It would require a full study using our Base model (Eq. 2) in place of the sample-based asymmetric modeling as part of the BBC simulations.

Nonetheless, it is enlightening to study the expected mean stretch difference as a function of redshift when considering that the underlying SN stretch distribution follows either the BBC formalism or our Base drifting model. This is shown Fig. 8, where, for clarity we convert this difference in mean stretch x_1 to a difference in magnitude using $\alpha = 0.156$ (Scolnic et al. 2018).

We see that the amplitude of the modeling difference is a few tens of millimag, which corresponds to the expected bias affecting SNe Ia impacted by sample selection effects. For comparison, the amplitude of this effect is similar in scale to the effect exotic forms of dark energy could have on $\mu(z)$. Consequently, in the era of modern cosmology, where we aim at probing w_0 at a sub-percent level and w_a at the ten-percent precision (e.g., Ivezić et al. 2019), it is of paramount importance to further un-

derstand the exact modeling of the lightcurve parameters when using SNe Ia affected by Malmquist bias.

6. Conclusion

We have presented a study of the drift of the *intrinsic still up to debate I think. We’ve been using “underlying” for the most part of the paper...* SNe Ia stretch distribution as a function of redshift. We built a magnitude-limited SN Ia sample from the Pantheon dataset (Scolnic et al. 2018, SDSS, PS1 and SNLS), to which we added HST and SNfactory data from Rigault et al. (2018) for the high- and low-redshift bins. We only considered the SNe that have been discovered in the redshift range of each survey where selection effects are negligible, so that the observed SNe Ia stretches are random sampling of the true underlying distribution. This resulted in a 569 SN Ia fiducial sample (422 SNe when more conservative cuts were considered).

Following predictions made in Rigault et al. (2018), we introduced a redshift drift model which depends on the expected fraction of “young” and “old” SNe Ia as a function of redshift, each age population having its own *intrinsic* stretch distribution.

In addition to this “base” modeling, we have studied various distributions, including redshift independent models; we also studied the prediction from the “Beams with Bias Correction”, a Malmquist bias correction algorithm used by several recent SN Ia cosmological analyses, implemented as a per-sample asymmetric Gaussian distribution.

Our conclusions are the following:

1. Non-drifting models are excluded as *suitable* descriptions of the data *relative to our Base model This does not mean anything... Indeed. Better? This model, which which one? Now clearer?* assumes that: (1) the younger population has a unimodal Gaussian stretch distribution, while the older population stretch distribution is bimodal, one mode being the same as the young one; (2) the evolution of the relative fraction of younger and older SNe Ia follows the prediction made in Rigault et al. (2018).
2. Given 1., we conclude that the SNe Ia stretch is indeed redshift dependent, as previously suggested by e.g. Howell et al. (2007). This result is largely independent of details on each age-population modeling. *Indeed, and this should be stated first!*
3. *reread & rephrase: “assuming” is not excluded!* Models assuming survey-based asymmetric Gaussian distributions, as done, e.g., in the current implementation of the BBC, *is are* excluded to be good descriptions of the data *relative to our drifting model*. Hence, sample-based approach does not accurately account for redshift drift, unlike what was suggested by Scolnic & Kessler (2016) and Scolnic et al. (2018).
4. An inaccurate underlying stretch distribution model is estimated to bias the mean standardized magnitude of SNe Ia affected *by* selection effects at the order of a few percents. This is comparable in scale to the observational signature of exotic forms of dark energy and is therefore a significant source of systematic that should be carefully studied.
5. Given the current dataset, we suggest the use of the following stretch population model as a function of redshift:

$$X_1(z) = \delta(z) \times \mathcal{N}(\mu_1, \sigma_1^2) + (1 - \delta(z)) \times \left[a \times \mathcal{N}(\mu_1, \sigma_1^2) + (1 - a) \times \mathcal{N}(\mu_2, \sigma_2^2) \right] \quad (6)$$

with: $a = 0.51$, $\mu_1 = 0.37$, $\mu_2 = -1.22$, $\sigma_1 = 0.61$, $\sigma_2 = 0.56$ (see Table 2) and using the age-population drift modelization

$\delta(z)$ defined in Rigault et al. (2018) *too many R+18 everywhere!* with $K = 0.87$:

$$\delta(z) = \left(K^{-1} \times (1+z)^{-2.8} + 1 \right)^{-1}. \quad (7)$$

In this paper, we considered a simple Gaussian mixture modeling, but additional data free from significant Malmquist bias would enable us to refine it. We highlight note that samples at the low- and high-redshift ends of the Hubble diagram would be particularly helpful for this drifting analysis; fortunately this will soon be provided by the Zwicky Transient Facility (Bellm et al. 2019; Graham et al. 2019) and Subaru SNe Ia program (REF HERE ASK NICOLAS), respectively. *Suggestion of adding a reference to the upcoming See Chang paper with ≈ 25 SNe at $z > 1.2$*

Acknowledgements. This project has received funding from the European Research Council (ERC) under the European Union's Horizon 2020 research and innovation programme (grant agreement n 759194 - USNAC).

References

- Abbott, T. M. C., Allam, S., Andersen, P., et al. 2019, ApJ, 872, L30
- Aldering, G., Adam, G., Antilogus, P., et al. 2002, Proc. SPIE, 61
- Astier, P., Guy, J., Regnault, N., et al. 2006, A&A, 447, 31
- Aubourg, É., Tojeiro, R., Jimenez, R., et al. 2008, A&A, 492, 631
- Bazin, G., Ruhlmann-Kleider, V., Palanque-Delabrouille, N., et al. 2011, A&A, 534, A43
- Bellm, E. C., Kulkarni, S. R., Graham, M. J., et al. 2019, PASP, 131, 018002
- Betoule, M., Kessler, R., Guy, J., et al. 2014, A&A, 568, A22
- Brout, D., Scolnic, D., Kessler, R., et al. 2019, ApJ, 874, 150
- Burnham, K., Anderson, D., 2004, Sociological Methods & Research, 33, 2
- Campbell, H., D'Andrea, C. B., Nichol, R. C., et al. 2013, ApJ, 763, 88
- Childress, M., Aldering, G., Antilogus, P., et al. 2013, ApJ, 770, 108
- Childress, M. J., Wolf, C., & Zahid, H. J. 2014, MNRAS, 445, 1898
- D'Andrea, C. B., Gupta, R. R., Sako, M., et al. 2011, ApJ, 743, 172
- Dilday, B., Kessler, R., Frieman, J. A., et al. 2008, ApJ, 682, 262
- Feeney, S. M., Peiris, H. V., Williamson, A. R., et al. 2019, Phys. Rev. Lett., 122, 061105
- Freedman, W. L., Madore, B. F., Hatt, D., et al. 2019, ApJ, 882, 34
- Freedman, W. L., Madore, B. F., Hoyt, T., et al. 2020, arXiv e-prints, arXiv:2002.01550
- Frieman, J. A., Bassett, B., Becker, A., et al. 2008, AJ, 135, 338
- Graham, M. J., Kulkarni, S. R., Bellm, E. C., et al. 2019, PASP, 131, 078001
- Gupta, R. R., D'Andrea, C. B., Sako, M., et al. 2011, ApJ, 740, 92
- Guy, J., Astier, P., Baumont, S., et al. 2007, A&A, 466, 11
- Hamuy, M., Phillips, M. M., Suntzeff, N. B., et al. 1996, AJ, 112, 2391
- Hamuy, M., Trager, S. C., Pinto, P. A., et al. 2000, AJ, 120, 1479
- Hinton, S. R., Davis, T. M., Kim, A. G., et al. 2019, ApJ, 876, 15
- Howell, D. A., Sullivan, M., Conley, A., et al. 2007, ApJ, 667, L37
- Ivezić, Ž., Kahn, S. M., Tyson, J. A., et al. 2019, ApJ, 873, 111
- Jones, D. O., Riess, A. G., & Scolnic, D. M. 2015, ApJ, 812, 3 1
- Jones, D. O., Riess, A. G., Scolnic, D. M., et al. 2018, ApJ, 867, 108
- Jones, D. O., Scolnic, D. M., Riess, A. G., et al. 2018, ApJ, 857, 51
- Jones, D. O., Scolnic, D. M., Foley, R. J., et al. 2019, ApJ, 881, 19
- Kelly, P. L., Hicken, M., Burke, D. L., et al. 2010, ApJ, 715, 743
- Kessler, R., Becker, A. C., Cinabro, D., et al. 2009, ApJS, 185, 32
- Kessler, R., & Scolnic, D. 2017, ApJ, 836, 56
- Kim, Y.-L., Smith, M., Sullivan, M., et al. 2018, ApJ, 854, 24
- Kim, Y.-L., Kang, Y., & Lee, Y.-W. 2019, Journal of Korean Astronomical Society, 52, 181
- Knox, L., & Millea, M. 2019, arXiv e-prints, arXiv:1908.03663
- Lampeitl, H., Smith, M., Nichol, R. C., et al. 2010, ApJ, 722, 566
- Mannucci, F., Della Valle, M., Panagia, N., et al. 2005, A&A, 433, 807
- Mannucci, F., Della Valle, M., & Panagia, N. 2006, MNRAS, 370, 773
- Maoz, D., Mannucci, F., & Nelemans, G. 2014, ARA&A, 52, 107
- Neill, J. D., Sullivan, M., Balam, D., et al. 2006, AJ, 132, 1126
- Neill, J. D., Sullivan, M., Howell, D. A., et al. 2009, ApJ, 707, 1449
- Pan, Y.-C., Sullivan, M., Maguire, K., et al. 2014, MNRAS, 438, 1391
- Perlmutter, S., Aldering, G., Goldhaber, G., et al. 1999, ApJ, 517, 565
- Perrett, K., Balam, D., Sullivan, M., et al. 2010, AJ, 140, 518
- Planck Collaboration, Aghanim, N., Akrami, Y., et al. 2018, arXiv e-prints, arXiv:1807.06209
- Poulin, V., Smith, T. L., Karwal, T., et al. 2019, Phys. Rev. Lett., 122, 221301
- Reid, M. J., Pesce, D. W., & Riess, A. G. 2019, arXiv e-prints, arXiv:1908.05625
- Rest, A., Scolnic, D., Foley, R. J., et al. 2014, ApJ, 795, 44
- Riess, A. G., Filippenko, A. V., Challis, P., et al. 1998, AJ, 116, 1009
- Riess, A. G., Macri, L., Casertano, S., et al. 2009, ApJ, 699, 539
- Riess, A. G., Macri, L. M., Hoffmann, S. L., et al. 2016, ApJ, 826, 56
- Riess, A. G., Casertano, S., Yuan, W., et al. 2018, ApJ, 861, 126
- Riess, A. G., Casertano, S., Yuan, W., et al. 2019, ApJ, 876, 85
- Rigault, M., Copin, Y., Aldering, G., et al. 2013, A&A, 560, A66
- Rigault, M., Aldering, G., Kowalski, M., et al. 2015, ApJ, 802, 20
- Rigault, M., Brinnel, V., Aldering, G., et al. 2018, arXiv:1806.03849
- Rodney, S. A., Riess, A. G., Strolger, L.-G., et al. 2014, AJ, 148, 13
- Roman, M., Hardin, D., Betoule, M., et al. 2018, A&A, 615, A68
- Rose, B. M., Garnavich, P. M., & Berg, M. A. 2019, ApJ, 874, 32
- Rubin, D., Aldering, G., Barbary, K., et al. 2015, ApJ, 813, 137
- Rubin, D., & Hayden, B. 2016, ApJ, 833, L30
- Sako, M., Bassett, B., Becker, A., et al. 2008, AJ, 135, 348
- Scannapieco, E., & Bildsten, L. 2005, ApJ, 629, L85
- Scolnic, D., Rest, A., Riess, A., et al. 2014, ApJ, 795, 45
- Scolnic, D., & Kessler, R. 2016, ApJ, 822, L35
- Scolnic, D. M., Jones, D. O., Rest, A., et al. 2018a, ApJ, 859, 101
- Scolnic, D., Perlmutter, S., Aldering, G., et al. 2019, Astro2020: Decadal Survey on Astronomy and Astrophysics, 2020, 270
- Shariff, H., Jiao, X., Trotta, R., et al. 2016, ApJ, 827, 1
- Strolger, L.-G., Riess, A. G., Dahlen, T., et al. 2004, ApJ, 613, 200
- Sullivan, M., Le Borgne, D., Pritchet, C. J., et al. 2006, ApJ, 648, 868
- Sullivan, M., Conley, A., Howell, D. A., et al. 2010, MNRAS, 406, 782
- Tasca, L. A. M., Le Fèvre, O., Hathi, N. P., et al. 2015, A&A, 581, A54
- Wiseman, P., Smith, M., Childress, M., et al. 2020, arXiv e-prints, arXiv:2001.02640
- Wong, K. C., Suyu, S. H., Chen, G. C.-F., et al. 2019, arXiv e-prints, arXiv:1907.04869